

SCIENTIFIC ARTICLE

The Protective Effects of Parathyroid Hormone (1-34) on Cartilage and Subchondral Bone Through Down-Regulating JAK2/STAT3 and WNT5A/ROR2 in a Collagenase-Induced Osteoarthritis Mouse Model

Li-tao Shao, MD, PhD^{1,2} , Yu Gou, MD, PhD³, Jia-kang Fang, MD², Yun-peng Hu, MD², Qiang-qiang Lian, MD², Zhou Yang, MD², Yu-ying Zhang, MD², Yu-dan Wang, MD², Fa-ming Tian, MD, PhD², Liu Zhang, MD, PhD^{1,4} 

¹Department of Orthopedic Surgery, Hebei Medical University, Shijiazhuang, ²Medical Research Center, Hebei Key Laboratory for Organ Fibrosis, North China University of Science and Technology, Tangshan, ³Department of Orthopedic Surgery, Tianjin Hospital, Tianjin University, Tianjin and ⁴Department of Orthopedic Surgery, Emergency General Hospital, Beijing, China

Objective: To assess the effects of PTH (1-34) on bone and cartilage metabolism in a collagenase-induced mouse model of osteoarthritis (OA) and examine whether PTH (1-34) affects the expression of JAK2/STAT3 and WNT5A/ROR2 in this process.

Methods: Eighteen 12-week-old male C57Bl/6 mice were randomly assigned into three groups as follows: sham group (Group A), the collagenase + saline injection group (Group B), and the collagenase + PTH (1-34) treatment group (Group C). Collagenase was injected (intra-articular) into the knee joint of Group B and C. The PTH (1-34)-treatment was started at 6 weeks after the operation and lasted for 6 weeks. Cartilage pathology was evaluated by gross visual, histological, and immunohistochemical assessments. Subchondral bone was evaluated by microcomputed tomography (micro-CT) and immunohistochemical analyses.

Results: The OARSI macroscopic and microscopic scores of Group B were higher than those of Group A ($P = 0.026$; $P = 0.002$, respectively). Group C showed statistically significant differences in macroscopic and microscopic scores from Group B ($P = 0.041$; $P = 0.008$, respectively). The results showed that the Col-II and AGG expression levels in the cartilage tissue were significantly lower in Group B than Group A ($P < 0.001$; $P = 0.008$, respectively). The Col-II and AGG expression levels were significantly higher in Group C than Group B ($P = 0.009$; $P = 0.014$, respectively). MMP-13, ADAMTS-4, Caspase-3, P53, and Bax expression levels were significantly higher in Group B than the Group A ($P < 0.001$; $P < 0.001$; $P = 0.04$; $P < 0.001$; $P = 0.005$, respectively); however, the cartilage tissue in Group C showed significantly less ADAMTS-4, MMP-13, Caspase-3, P53, and Bax expression than Group B ($P < 0.001$, $P < 0.001$, $P = 0.044$; $P = 0.002$; $P = 0.005$, respectively). Over-expressed JAK2/STAT3 and WNT5A/ROR2 were observed in both cartilage and subchondral bone in this model; however, these changes were prevented by PTH (1-34) treatment. These parameters (bone mineral density, bone volume ratio, trabecular bone pattern factor, and structure model index) of micro-CT indicated subchondral bone loss and architecture changes in Group B, but improvements in these parameters in Group C.

Conclusions: PTH (1-34) exhibits protective effects on both cartilage and subchondral bone in a collagenase-induced OA mouse model, and it may be involved in down-regulating the expression of JAK2/STAT3 and WNT5A/ROR2.

Key words: Cartilage; JAK2; Osteoarthritis; Parathyroid hormone; Subchondral bone

Address for correspondence Liu Zhang, MD, PhD, Department of Orthopedic Surgery, Emergency General Hospital, Xibahenanli 29, Chaoyang dis, Beijing, China 100028 Tel: 86-10-64662308; Fax: +86-315-3725861; Email: zhliu130@sohu.com and Fa-ming Tian, MD, PhD, Medical Research Center, North China University of Science and Technology, Tangshan, China 063000 Tel: +86-0315-8808011; Fax: +86-315-8805560; Email: tfm9911316@163.com
Received 6 July 2020; accepted 18 March 2021

Introduction

Osteoarthritis (OA) is the leading cause of disability in the elderly population worldwide, which results in an enormous socio-economic burden¹. At present, the pathogenesis of OA is not clear and there is no effective drug to delay the progression of OA. Therefore, it is important to explore the mechanism of OA and find the drugs to delay OA.

OA is the most common joint disease that influences the whole joint, including the articular cartilage and subchondral bone²⁻⁵. Increasing evidence indicates that cartilage damage is closely related to subchondral bone degeneration in the development of OA^{1,2,6,7}. Studies have shown that changes of subchondral bone occur before pathological changes of articular cartilage in the pathogenesis of OA^{8,9}. Poor subchondral bone conditions may promote cartilage degradation^{6,10,11}. Changes in subchondral bone include increased remodeling (bone loss) and altered subchondral trabecular bone architecture in the early stage of OA and subchondral densification (osteophytes) in the late stage of OA¹². Changes in the articular cartilage include extracellular matrix (ECM) homeostasis imbalance and chondrocyte apoptosis, which gradually lead to surface irregularities, fissures, and even denudation of cartilage¹³⁻¹⁶. Cartilage and subchondral bone degeneration are important causes of OA. These pathological changes provide a direction for us to find drugs to treat OA.

The American Academy of Orthopaedic Surgeons (AAOS) has formulated OA treatment guidelines and recommends the use of celecoxib (CLX) for the relief of pain and other symptoms; however, clear clinical evidence that CLX can delay the progress of OA is not available. Therefore, it is particularly important to find drugs that delay the progression of OA. Intriguingly, recent research found that parathyroid hormone (PTH) (1-34), which is used for the treatment of osteoporosis, may have a therapeutic benefit in the treatment of OA^{17,18}. PTH (1-34) has been reported to not only maintain bone mass but also improve articular cartilage surface architecture and integration^{18,19}. Previous studies have revealed that PTH (1-34) activates multiple pathways by binding to parathyroid hormone/parathyroid hormone-related peptide receptor (PTH1R) and thus exerts important effects on chondrocytes, osteocytes, osteoblasts, and osteoclasts^{17,20-22}. Therefore, PTH (1-34) may represent a drug that delays OA. However, the effects of PTH (1-34) on cartilage and subchondral bone in collagenase-induced OA mouse models have not been previously reported.

The mechanism of action of PTH (1-34) on cartilage and subchondral bone of OA is unclear. Growing evidence suggests that JAK2 and STAT3 are over-expressed in cartilage and subchondral bone during the development of OA²³⁻²⁶. Previous studies have shown that the expression of WNT5A is up-regulated in cartilage degradation and subchondral bone changes in the pathogenesis of OA²⁷⁻²⁹. The increased JAK2/STAT3 and WNT5A may be involved in the occurrence and development of OA. However, in terms of

current knowledge, the effect of PTH (1-34) on the expression of JAK2/STAT3 and WNT5A/ROR2 has not been reported.

Therefore, the purposes of the present study were: (i) to observe the effect of collagenase on the knee joint in mice; (ii) to evaluate the effects of PTH (1-34) on cartilage and subchondral bone in a collagenase-induced OA mouse model; and (iii) to provide some primary data focused on the expression of the JAK2/STAT3 and WNT5A/ROR2 pathways in this process.

Materials and Methods

Animals

The experiment was approved by the Institutional Animal Care and Use Committee. Eighteen 12-week-old male C57Bl/6 mice (Vital River Experimental Animal Technical Co., Ltd., Beijing, China) were fed a standard rodent diet and housed in the Medical Research Animal Center. The mice were randomly assigned into three groups as follows: sham group (Group A), the collagenase + saline injection group (Group B), and the collagenase + PTH (1-34) treatment group (Group C). All mice were housed under standard laboratory conditions in a temperature-controlled room (21 °C ± 1 °C) and maintained on a 12 h light/12 h dark cycle.

Induction of Experimental OA and Drug Treatment

The induction of experimental OA was carried out using previously validated procedures³⁰. Briefly, collagenase (type VII, Sigma-Aldrich) was injected (intra-articular) into the patellar ligament of the Group B and C using a microsyringe on days 0 and 2 and saline was administered to Group A. Animals in Group C received subcutaneous injections of 40 µg/kg/day (5 days weekly) of PTH (1-34) (Sigma-Aldrich Corp, US). Mice in Group A received the same surgical procedures as the collagenase injection mice but the microsyringe did not puncture the patellar ligament and then the skin was closed. This treatment was started at 6 weeks after the operation and lasted for 6 weeks. Finally, all animals were euthanized with CO₂ to harvest the entire knee joint. The experimental process is shown in Fig. 1.

Macroscopic Findings

After separating at the joints, both the femur and tibia were cleaned and the appearance was recorded with a digital camera (Canon, Tokyo, Japan). Gross morphologic grading of the medial tibias was examined according to the Osteoarthritis Research Society International (OARSI) score system as follows: grade 0 (normal cartilage surface); grade 1 (surface roughening); grade 2 (fibrillation and small cartilage erosions); grade 3 (large erosions extending down to the subchondral bone); and grade 4 (larger erosions down to the subchondral bone)³¹.

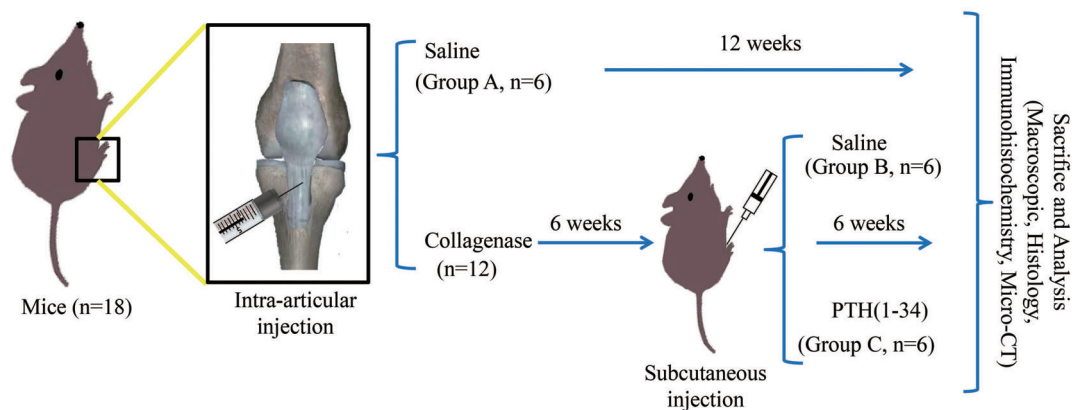


Fig 1 Experimental flowchart. Eighteen 12-week-old male C57Bl/6 mice were randomly assigned to three groups. Sham group (Group A, n = 6) underwent a sham surgical procedure. The collagenase + saline injection group (Group B, n = 6) and the collagenase + PTH (1-34) treatment group (Group C, n = 6) were injected collagenase. Saline and PTH (1-34) injection was started at 6 weeks after the operation and lasted for 6 weeks. Finally, all animals were euthanized and analyzed. The analysis included macroscopic, histology, immunohistochemistry, and micro-computed tomography (micro-CT). PTH, parathyroid hormone.

Histology

The left knees were fixed in 4% formalin solution for 48 h and decalcified with 10% Na₂EDTA (PH = 7.4) for 7 weeks. The tibias and femurs were dehydrated, embedded in paraffin, and cut to 6 μm in thickness. The coronal sections from each sample were stained with toluidine blue. Then, section images were recorded under an optical microscope (Olympus BX53, Olympus, Japan). Semi-quantitative histopathological analyses established five characteristics according to the OARSI score system: articular cartilage structure, chondrocyte density, cell cloning, tidemark integrity, and interterritorial toluidine blue³².

Immunohistochemical Assessments

Immunohistochemistry was performed with primary antibodies to collagen type II (Col-II) (1:300; DSHB Hybridoma Product II-II6B3, Linsenymer TF), metalloproteinase-13 (MMP-13) (1:1000; Gene Tex Inc., USA), aggrecan (AGG) (1:200; Abbotec LLC, USA), a disintegrin and metalloproteinase with thrombospondin motifs type 4 (ADAMTS-4) (1:500; Abclonal, China), Caspase-3 (1:300; Boster Co. Ltd., China), Bax (1:200; Proteintech, China), P53 (1:200; Proteintech, China), WNT5A (1:100; Abcam, UK), ROR2 (1:200; Affinity Biosciences, USA), JAK2 (1:100; Proteintech, China), and STAT3 (1:100; Proteintech, China). Briefly, all sections were deparaffinized, rehydrated and repaired with 0.05% trypsin, endogenous peroxidases were inactivated with H₂O₂ at room temperature for 10 min, and incubation was performed with the previous target protein overnight at 4°C. Finally, the remaining experimental procedures were performed using the PV-6000 DAB detection kit and the ZLI-9018 DAB kit (both from ZSGB-BIO Corp., China). In the cartilage tissue of the tibia plateau, the average intensity of optical density (IOD), given in IOD/mm², was

defined as the sum of the integrated optical density divided by the area of cartilage tissue in the region of interest (ROI) under a magnification of 10×. In subchondral bone, the IOD was evaluated under a magnification of 40×. All sections were measured by Image Pro Plus (IPP) version 6.0 software (Media Cybernetics, Rockville, Maryland, USA).

Micro-Architecture Parameters of Subchondral Bone

To investigate alterations in the subchondral bone micro-architecture, the left knees were imaged using micro-computed tomography (micro-CT) (SkyScan1176 Software: Version 1.1, build 6, Bruker, Kontich, Belgium), with a resolution of 9 μm per voxel. Data were collected at 50 KeV of energy, with a 270-μA current and 8.96580-μm cubic resolution. For the bone histomorphometry analysis, the ROI was defined as the trabecular bone of the tibia subchondral bone at the cross-sectional level, excluding the cortical shell^{6,25}. The bone mineral density (BMD), bone volume ratio (BV/TV), trabecular bone pattern factor (Tb.Pf), and Structure Model Index (SMI) were calculated to describe the bone mass and structure.

Statistical Analysis

All data were expressed as the mean ± standard deviation (SD), and all statistical analyses were performed using SPSS version 19.0 (SPSS Inc., Chicago, IL, USA). One-way analysis of variance (ANOVA) was performed to confirm the differences in data with a normal distribution among groups, and it was followed by Fisher's least significant difference (LSD) test or Dunnett's T3 test to perform pairwise comparisons. The differences in OARSI scores among groups were determined with the Kruskal-Wallis H test, and pairwise comparisons were performed with the Mann-Whitney U test. The level of statistical significance was established at *P* < 0.05.

Results

OARSI Scoring of Cartilage

The experimental operation significantly impaired the articular cartilage of the medial tibial plateau (Fig. 2). The OARSI macroscopic scores of Group B were higher than those of Group A (2.2 ± 0.8 in Group B vs 1 ± 0.6 in Group A, Group B significantly increased [120%], $P = 0.026$). Group C showed statistically significant differences in macroscopic score from Group B (1.2 ± 0.4 in Group C vs 2.2 ± 0.8 in Group B, Group C significantly decreased [45.5%], $P = 0.041$).

The histological evaluation of the medial tibial plateau showed that the cartilage of Group B was severely injured (Fig. 3). The total scores in Group B were significantly higher than those in Group A (10 ± 1.8 in Group B vs 3.7 ± 2 in Group A, Group B significantly increased [170.3%], $P = 0.002$), while those of Group C were lower than those of Group B (6.7 ± 1 in Group C vs 10 ± 1.8 in Group B, Group C significantly decreased [33%], $P = 0.008$).

Immunohistochemical Analysis of Cartilage

Expression of the following proteins in the cartilage samples was evaluated by an immunohistochemical assay: Col-II, AGG, MMP-13, ADAMTS-4, Caspase-3, P53, Bax, JAK2, STAT3, WNT5A, and ROR2. Proteins expressed in each cartilage sample and the average IOD are shown in Figs 4–7.

Col-II and AGG Expression Levels

The results showed that the Col-II and AGG expression levels in the cartilage tissue were significantly lower in Group B than Group A (285462.8 ± 163776.3 in Group B vs 1089319.5 ± 424125.4 in Group A, the Group B significantly decreased [73.8%], $P < 0.001$; 21558.3 ± 14394 in Group B vs 108705.1 ± 64813.9 in Group A, the Group B significantly decreased [80.2%], $P = 0.008$, respectively). The Col-II and AGG expression levels were significantly higher in Group C than Group B (796834.5 ± 439610.3 in Group C vs 285462.8 ± 163776.3 in Group B, Group C significantly increased [179.1%], $P = 0.009$; 100213.5 ± 53506.2 in Group

C vs 21558.3 ± 14394 in Group B, Group C significantly increased [364.8%], $P = 0.014$, respectively).

ADAMTS-4 and MMP-13 Expression Levels

ADAMTS-4 and MMP-13 were mainly expressed in the cartilage underneath the damaged area in the cartilage. ADAMTS-4 expression level was significantly higher in Group B than Group A (129716.8 ± 40346 vs 10186.6 ± 6466.4 , Group B significantly increased [1173.4%], $P < 0.001$); however, the cartilage tissue in Group C showed significantly less ADAMTS-4 expression than Group B (29208.3 ± 18815.4 vs 129716.8 ± 40346 , Group C significantly decreased [77.5%], $P < 0.001$). The mean MMP-13 expression level was 289897.5 ± 108314.4 in Group B and 62795.7 ± 33870.6 in Group A, this increase (361.7%) was also significant; however, Group C (57332.5 ± 31975.7) showed significantly less expression than Group B (Group C significantly decreased [80.2%], $P < 0.001$).

Caspase-3, P53, and Bax Positive Expression

Caspase-3, P53, and Bax positive cells were observed in the area beneath damaged cartilage, while the Caspase-3, P53, and Bax levels were significantly higher in Group B than Group A (210626.4 ± 123946.8 in Group B vs 28690.6 ± 16985.3 in Group A, Group B significantly increased [634.1%], $P = 0.04$; 128087.3 ± 69480.9 in Group B vs 10737.2 ± 8256.6 in Group A, Group B significantly increased [1092.9%], $P < 0.001$; 14881.2 ± 5702.7 in Group B vs 2012.2 ± 1626.8 in Group A, Group B significantly increased [639.5%], $P = 0.005$, respectively). The Caspase-3, P53, and Bax levels were significantly lower in Group C than Group B (33348 ± 19677 in Group C vs 210626.4 ± 123946.8 in Group B, Group C significantly decreased [84.2%], $P = 0.044$; 38388.9 ± 14088.4 in Group C vs 128087.3 ± 69480.9 in Group B, Group C significantly decreased [70%], $P = 0.002$; 2235.6 ± 2011 in Group C vs 14881.2 ± 5702.7 in Group B, the Group C significantly decreased [85%] $P = 0.005$, respectively).

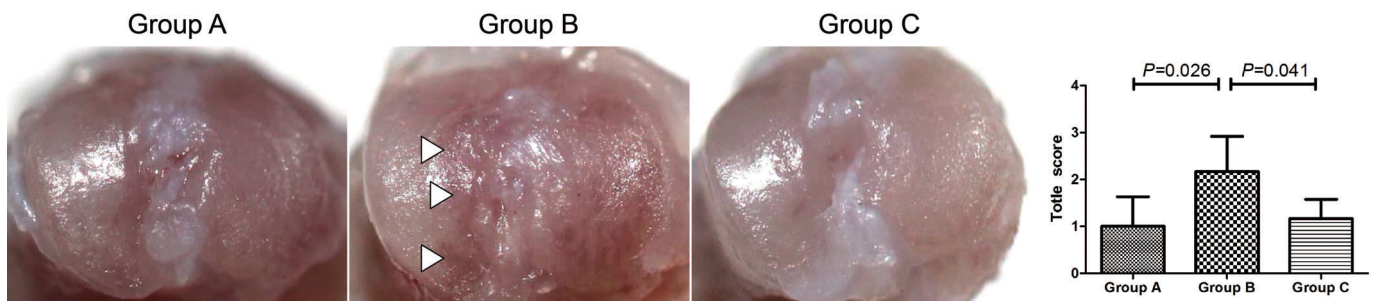


Fig 2 Macroscopic view of the right tibial plateau of the samples, and OARSI macroscopic scoring between groups. White arrows show damage to the tibial plateau. Data are presented as the mean \pm SD. Group A, sham group; Group B, the collagenase + saline injection group; Group C, the collagenase + PTH (1-34) treatment group. PTH, parathyroid hormone.

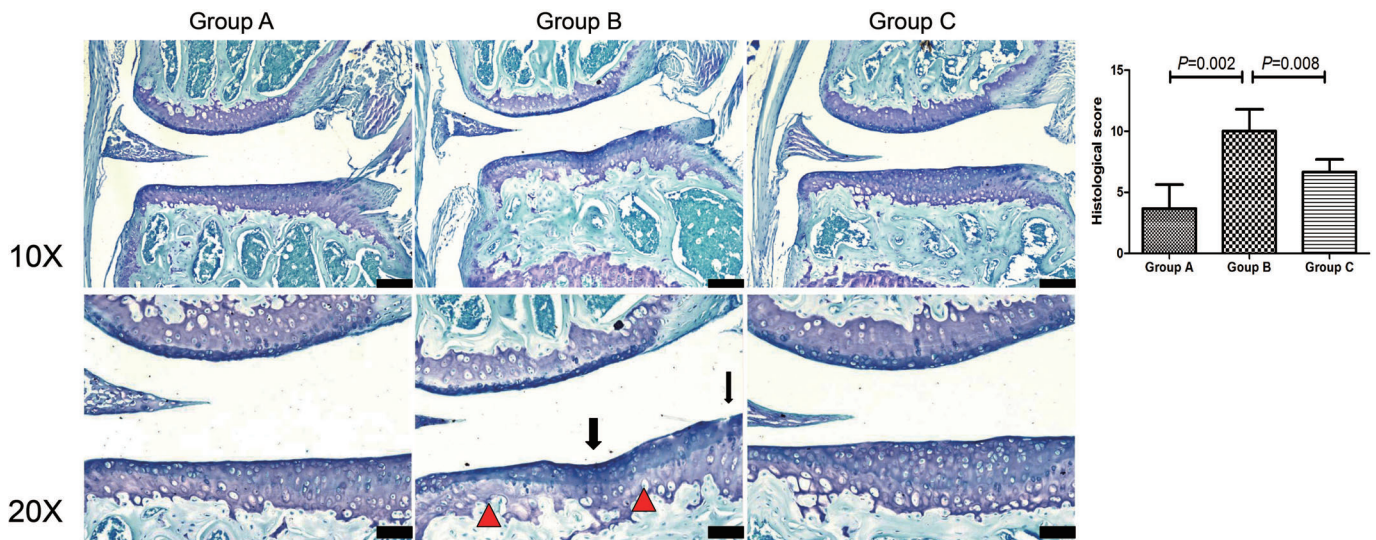


Fig 3 OARSI microscopic scoring between groups (toluidine blue staining). Toluidine blue stain of the medial tibial plateau of samples. Black arrows indicate lesions of the tibial plateau, and red triangle indicate matrix loss. Data are presented as the mean \pm SD. Group A, sham group; Group B, the collagenase + saline injection group; Group C, the collagenase + PTH (1-34) treatment group. PTH, parathyroid hormone.

JAK2 and STAT3 Expression Levels

The JAK2 and STAT3 expression levels in the cartilage tissue were significantly higher in Group B than Group A (64355.2 ± 43547.1 in Group A vs 7957.9 ± 6506.5 in Group B, Group B significantly increased [708.7%], $P = 0.002$; 101041 ± 43835.2 in Group B vs 18065.6 ± 16451.2 in Group A, Group B significantly increased [459.3%], $P = 0.012$, respectively) but was significantly lower in Group C than Group B (12448.2 ± 9161.5

in Group C vs 64355.2 ± 43547.1 in Group B, Group C significantly decreased [80.7%], $P = 0.003$; 28882.9 ± 18789 in Group C vs 101041 ± 43835.2 in Group B, Group C significantly decreased [71.4%], $P = 0.022$, respectively).

WNT5A and ROR2 Expression Levels

The WNT5A and ROR2 expression levels in the cartilage tissue were significantly higher in Group B than Group A

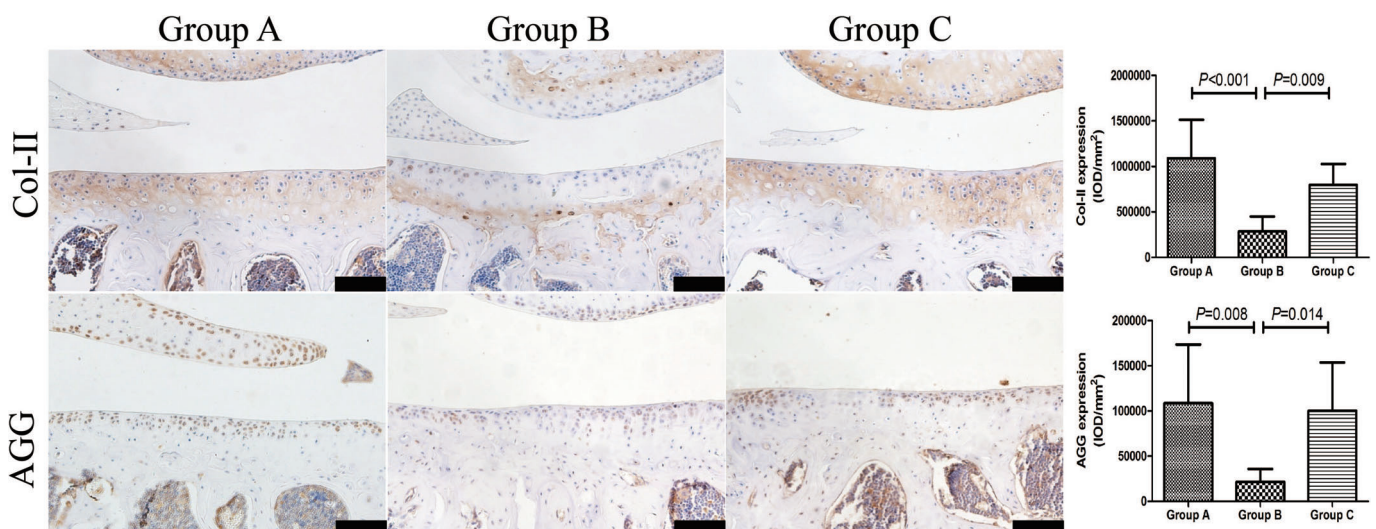


Fig 4 Immunohistochemical staining of groups (20 \times). This figure demonstrates the expression of collagen-II (Col-II) and aggrecan (AGG) in load-bearing areas of cartilage among groups. The positive expression of Col-II and AGG was defined as brown-yellow stain. Data are presented as the mean \pm SD. Scale bars = 100 μ m. Group A, sham group; Group B, the collagenase + saline injection group; Group C, the collagenase + PTH (1-34) treatment group. PTH, parathyroid hormone.

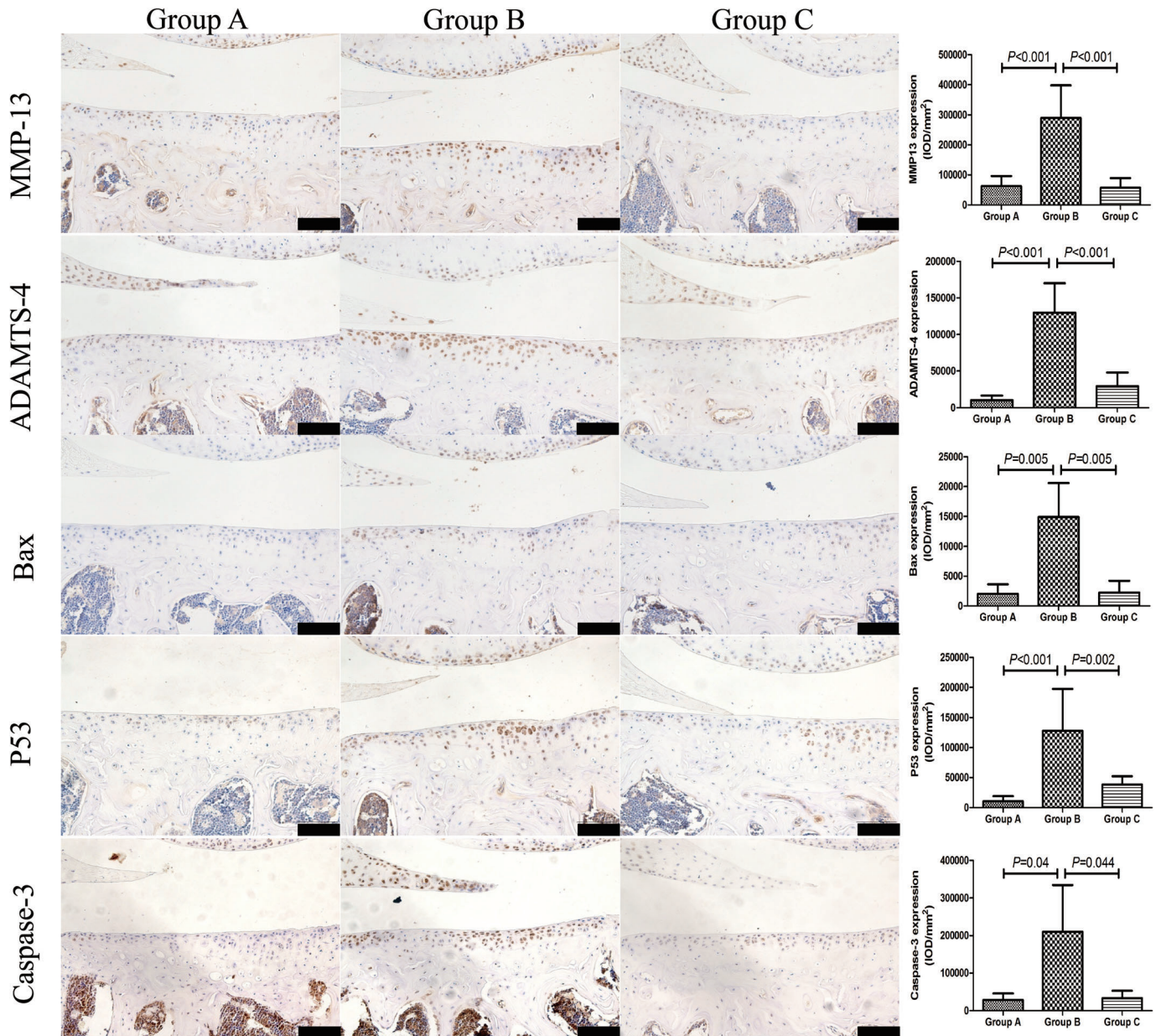


Fig 5 Immunohistochemical staining of groups (20x). This figure demonstrates the expression of matrix metalloproteinase-13 (MMP-13), a disintegrin and metalloproteinase with thrombospondin motifs-4 (ADAMTS4), Bax, P53, and Caspase-3 in load-bearing areas of cartilage among groups. The positive expression of MMP-13, ADAMTS4, Bax, P53, and Caspase-3 was defined as brown-yellow stain. Data are presented as the mean \pm SD. Scale bars = 100 μ m. Group A, sham group; Group B, the collagenase + saline injection group; Group C, the collagenase + PTH (1-34) treatment group. PTH, parathyroid hormone.

(12205.9 \pm 1824 in Group B vs 5270.5 \pm 4698.9 in Group A, Group B significantly increased [131.6%], $P = 0.006$; 4942.9 \pm 1534.9 in Group B vs 1729.7 \pm 415.9 in Group A, Group B significantly increased [185.8%], $P = 0.008$, respectively) but significantly lower in Group C than Group B (6885.6 \pm 4101 in Group C vs 12205.9 \pm 1824 in Group B, Group C significantly decreased [43.6%], $P = 0.027$; 2234.6 \pm 844.1 in Group C vs 4942.9 \pm 1534.9 in Group B,

Group C significantly decreased [54.8%], $P = 0.016$, respectively).

Immunohistochemical Analysis of Subchondral Bone

The JAK2 and STAT3 expression levels in the subchondral bone were significantly higher in Group B than Group A (32780.8 \pm 9239.5 in Group B vs 13996 \pm 1897.9 in Group A, Group B significantly increased [134.2%],

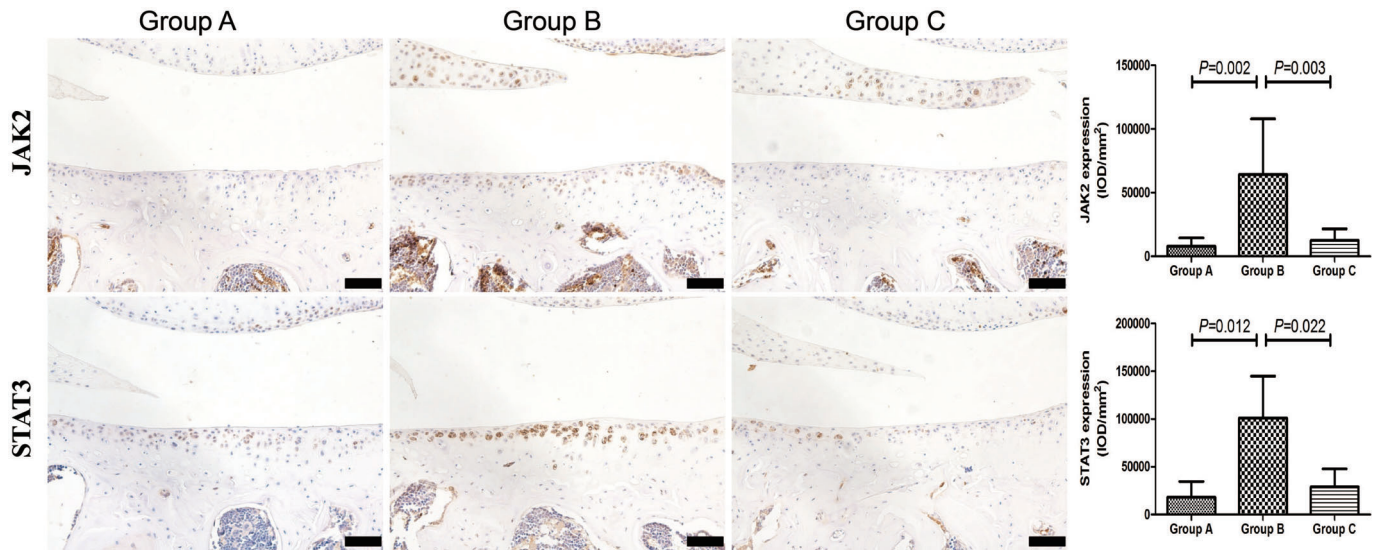


Fig 6 Immunohistochemical staining of groups (20 \times). This figure demonstrates the expression of JAK2 and STAT3 in load-bearing areas of cartilage among groups. The positive expression of JAK2 and STAT3 was defined as brown-yellow stain. Data are presented as the mean \pm SD. Scale bars = 100 μ m. Group A, sham group; Group B, the collagenase + saline injection group; Group C, the collagenase + PTH (1-34) treatment group. PTH, parathyroid hormone.

$P < 0.001$; 10175.2 ± 5256.5 in Group B vs 2172.8 ± 1267.5 in Group A, Group B significantly increased [368.3%], $P = 0.002$, respectively) but were significantly lower in Group C than Group B (8802.6 ± 2192.7 in Group C vs 32780.8 ± 9239.5 in Group B, Group C significantly decreased [73.1%], $P < 0.001$; 1844.4 ± 872.6 in Group C vs

10175.2 ± 5256.5 in Group B, Group C significantly decreased [81.9%], $P = 0.001$, respectively) (Fig. 8).

The WNT5A and ROR2 expression levels in subchondral bone were significantly higher in Group B than Group A (3318.7 ± 1397.6 in Group B vs 635.7 ± 458 in Group A, Group B significantly increased [422.1%],

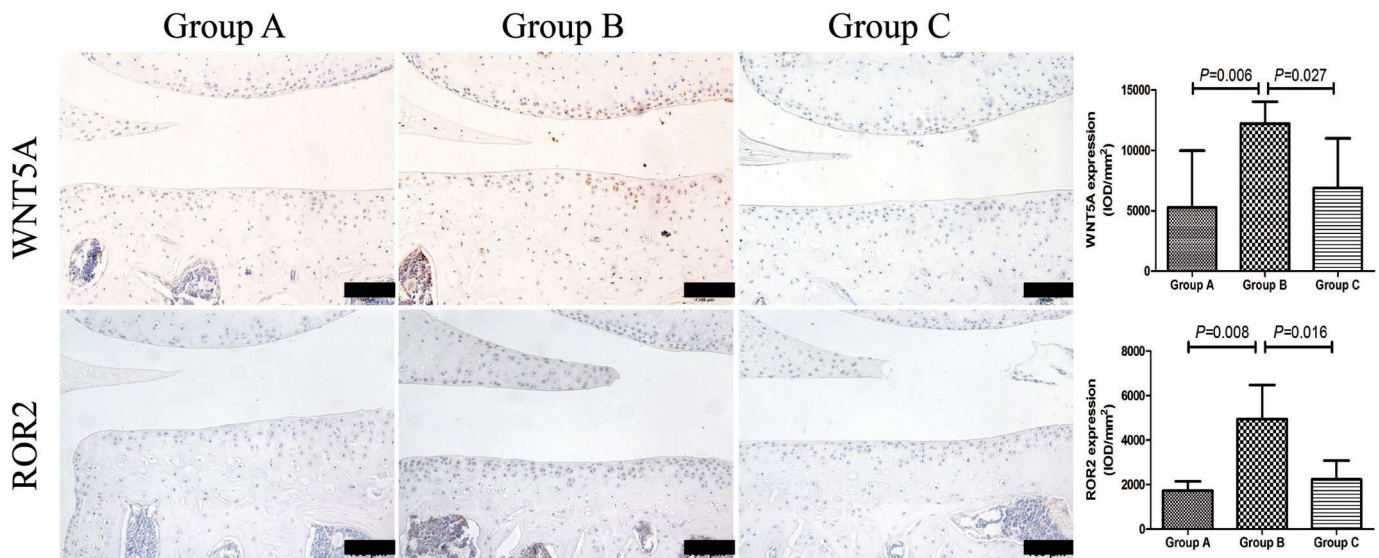


Fig 7 Immunohistochemical staining of groups (20 \times). This figure demonstrates the expression of WNT5A and ROR2 in load-bearing areas of cartilage among groups. The positive expression of WNT5A and ROR2 was defined as brown-yellow stain. Data are presented as the mean \pm SD. Scale bars = 100 μ m. Group A, sham group; Group B, the collagenase + saline injection group; Group C, the collagenase + PTH (1-34) treatment group. PTH, parathyroid hormone.

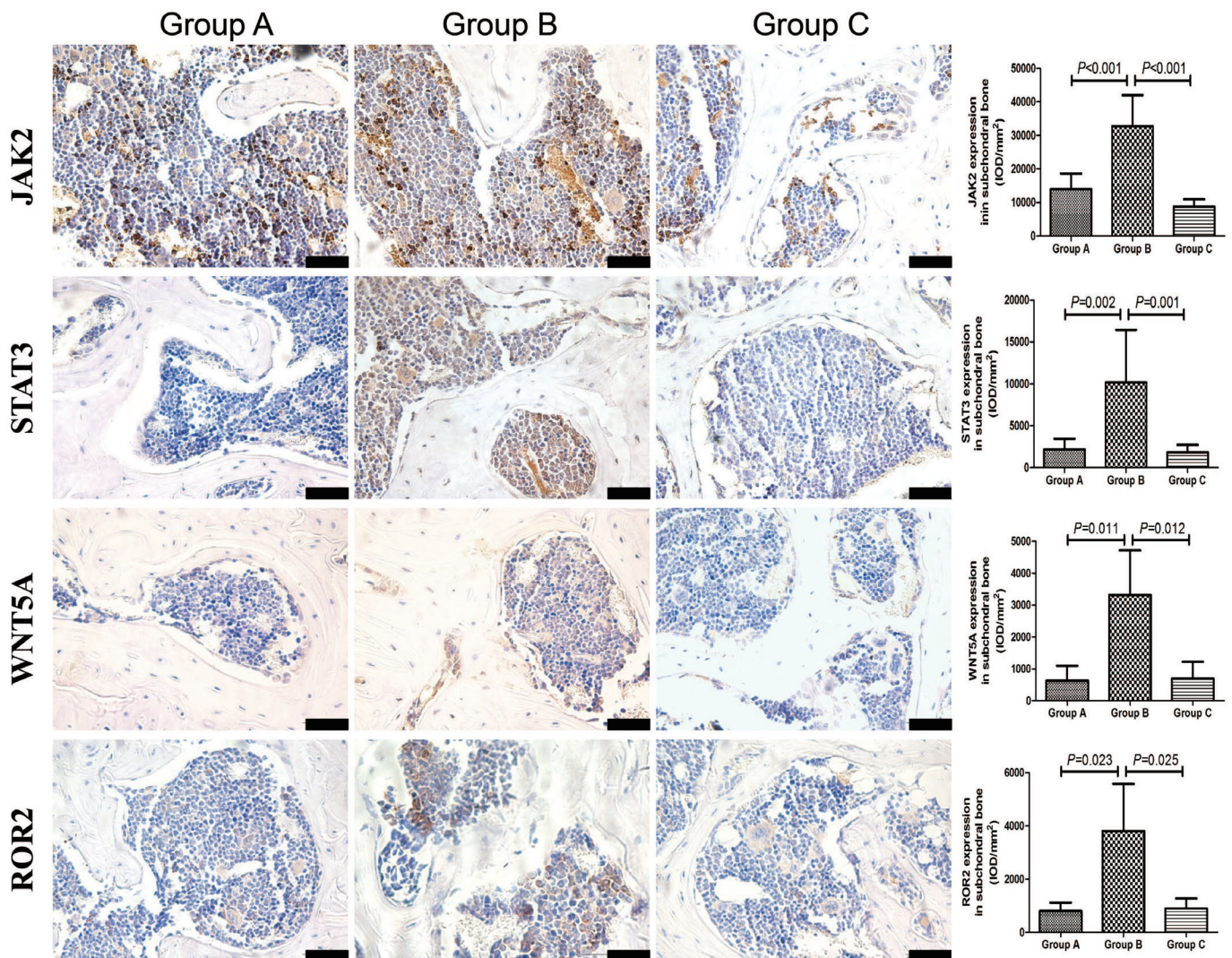


Fig 8 Immunohistochemical staining of groups (40 \times). This figure demonstrates the expression of JAK2, STAT3, WNT5A, and ROR2 in load-bearing areas of subchondral bone among groups. The positive expression of JAK2, STAT3, WNT5A, and ROR2 was defined as brown-yellow stain. Data are presented as the mean \pm SD. Scale bars = 50 μ m. Group A, sham group; Group B, the collagenase + saline injection group; Group C, the collagenase + PTH (1-34) treatment group. PTH, parathyroid hormone.

$P = 0.011$; 3806.4 ± 1780.8 in Group B vs 802.3 ± 320.3 in Group A, Group B significantly increased [374.5%], $P = 0.023$, respectively) but were significantly lower in Group C than Group B (693.6 ± 525.7 in Group C vs 3318.7 ± 1397.6 in Group B, Group C significantly decreased [79.1%], $P = 0.012$; 899.4 ± 380.2 in Group C vs 3806.4 ± 1780.8 in Group B, Group C significantly decreased [76.4%], $P = 0.025$, respectively) (Fig. 8).

Micro-architecture Parameters of Subchondral Bone

As shown in Fig. 9, the results indicated that the BMD and BV/TV were significantly lower in Group B than Group A (448.2 ± 27.1 mg/cm² in Group B vs 517.1 ± 40.2 mg/cm² in Group A, Group B significantly

decreased [13.3%], $P = 0.003$; $25.6\% \pm 2.6\%$ in Group B vs $31.7\% \pm 4.2\%$ in Group A, Group B significantly decreased [19.5%], $P = 0.009$, respectively) but were significantly higher in Group C than Group B (597.6 ± 30.1 mg/cm² in Group C vs 448.2 ± 27.1 mg/cm² in Group B, Group C significantly increased [33.3%], $P < 0.001$; $40.7\% \pm 3.7\%$ in Group C vs $25.6\% \pm 2.6\%$ in Group B, Group C significantly increased [59.2%], $P < 0.001$, respectively). Other subchondral bone micro-architecture parameters (trabecular bone pattern factor (Tb.Pf) and structure model index (SMI)) indicated subchondral bone loss and architecture changes in Group B but significant improvements in bone loss and micro-architecture in the PTH (1-34) group.

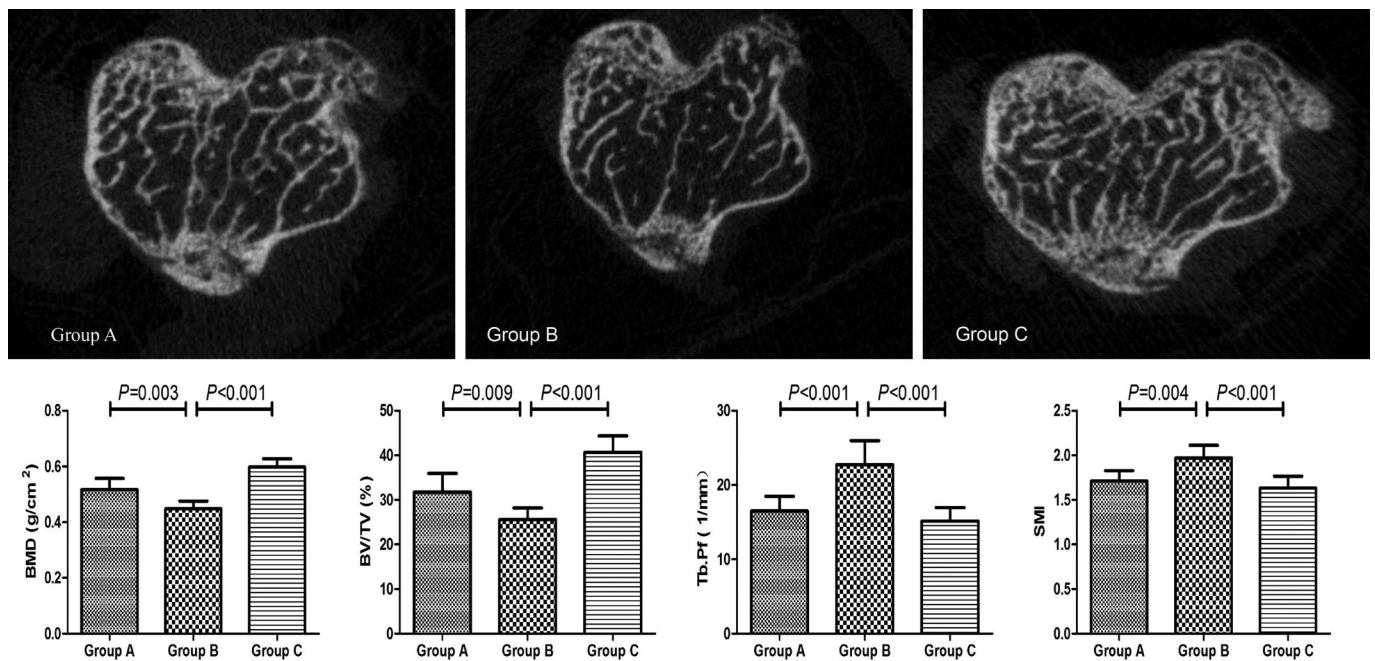


Fig 9 Histomorphometric parameters of subchondral bone by microcomputed tomography (micro-CT) analysis. Data are presented as the mean \pm SD. Group A, sham group; Group B, the collagenase + saline injection group; Group C, the collagenase + PTH (1-34) treatment group. PTH, parathyroid hormone.

Correlation Analysis

Significant negative correlations were observed between the expression of Col-II and the expression of JAK2, STAT3, WNT5A, and ROR2 ($r = 0.526, 0.53, 0.504, 0.643$, respectively; $P = 0.025, 0.024, 0.033, 0.004$, respectively); between the expression of Caspase-3 and the expression of JAK2, STAT3, WNT5A, and ROR2 ($r = 0.616, 0.72, 0.47, 0.75$, respectively; $P = 0.006, 0.001, 0.049, <0.001$, respectively); and between the expression of BMD and the expression of JAK2, STAT3, WNT5A, and ROR2 ($r = 0.632, 0.601, 0.509, 0.654$, respectively; $P = 0.005, 0.008, 0.031, 0.001$, respectively). Significant positive correlations were observed between SMI and JAK2, WNT5A, and ROR2 ($r = 0.724, 0.566, 0.568$, respectively; $P = 0.001, 0.014, 0.014$, respectively).

Discussion

In the present study, we found that PTH (1-34) plays an important role in maintaining cartilage metabolism, reducing chondrocyte apoptosis and inhibiting subchondral bone microstructure deterioration in a collagenase-induced OA mouse model by down-regulating the expression of JAK2/STAT3 and WNT5A/ROR2.

This study demonstrates that Group B experienced cartilage damage, including the formation of fissures and defects on the surface of the cartilage and the loss of local matrix. These findings were consistent with some previous studies^{30,33,34}. We observed that systemic application of PTH (1-34) directly prevented cartilage damage progression. In

our research, PTH (1-34) treatment dramatically down-regulated MMP-13 and ADAMTS-4 expression in the cartilage and up-regulated the expression of Col-II and AGG in the cartilage. Col-II is an important component in cartilage that can maintain the elastic strength and smooth surface of the entire cartilage⁷. AGG is also one of the main components of the extracellular matrix, and its main role is to bind water molecules, thereby providing shock absorption and compression resistance for articular cartilage³⁵. MMP-13 and ADAMTS-4 are important catabolic enzymes responsible for the degradation of the extracellular matrix, and greater expression of these enzymes correlates to higher OA severity^{6,7}. The inhibition of MMP-13 and ADAMTS-4 were thought to have a protective effect on articular cartilage^{1,6}. Consistent with these assumptions, the present findings suggested that PTH (1-34) treatment can protect the integrity of the extracellular matrix in the progression of OA in this model. In addition, cartilage degeneration caused by chondrocyte apoptosis plays an important role in the development of OA^{36,37}. P53 is a transcriptional regulator that plays an important role in the initiation of apoptosis because it can stimulate Bax gene expression, thereby promoting apoptosis. Caspase-3 is also a key apoptotic executive factor. The expression of Caspase-3, P53, and Bax has been reported to be upregulated *via* OA models^{24,38}. In our study, we found that the expression of Caspase-3, P53, and Bax was upregulated in the collagenase-induced OA mouse model; however, these changes were prevented by the PTH (1-34) treatment. In brief, the findings of this study showed that

PTH (1-34) could preserve the balance of cartilage metabolism and decrease the apoptosis of chondrocytes in the OA model.

Recent observations have suggested that a loss of bone occurs in the early stage of OA¹². Bone loss in the subchondral bone may lead to abnormal stress on the cartilage, and the altered mechanics may lead to OA by changing the cartilage matrix or damaging the integrity of cartilage¹¹. In our study, bone mass decreased in Group B but was significantly increased in the PTH (1-34)-treated animals. Thus, previous results and the results of the current study support that PTH (1-34) may have a beneficial effect on cartilage by inhibiting subchondral bone remodeling and preserving subchondral bone micro-architecture^{6,7,39}.

To further study the mechanism of PTH (1-34) on cartilage and subchondral bone, we observed the expression of JAK2, STAT3, WNT5A, and ROR2 in the cartilage and subchondral bone.

JAK/STAT is an important family of intracellular signaling pathways, and the JAK2/STAT3 signaling pathway is involved in OA progress and over-expressed in OA cartilage and subchondral bone^{23,24}. Importantly, JAK2 and STAT3 are related to MMPs and Caspase-3 in primary chondrocytes^{40,41} and enhance osteocyte-mediated osteoclastic differentiation *in vitro*⁴² and mineralization disorder *in vivo*²³. These findings are consistent with early OA pathological features, including cartilage damage and bone mass loss. In the current study, JAK2 and STAT3 were over-expressed in OA cartilage and subchondral bone; however, PTH (1-34) down-regulated JAK2 and STAT3 expression in OA cartilage and subchondral bone. According to our study and other results, we presumed that increased JAK2 and STAT3 expression can lead to cartilage matrix damage (due to decreased Col-II), increased chondrocyte apoptosis (due to increased expression of Caspase-3), and subchondral bone structure changes (mainly caused by increased SMI and decreased BMD)^{23,24,40-43}, but PTH reversed these changes. Therefore, we speculate that the protective effect of cartilage and subchondral bone by PTH (1-34) may be due to down-regulating the expression of JAK2 and STAT3 in this OA model.

The Wnt family can be divided into two categories: the canonical class and the non-canonical class. Two of the best characterized non-canonical Wnt signaling pathways are the Wnt/Ca²⁺ and Wnt/planar cell polarity (PCP) pathways. Increasing evidence suggests that aberrant Wnt signaling contributes to cartilage damage and subchondral bone changes in OA^{29,44,45}. WNT5A expression was detected at

increased levels in OA cartilage^{28,46}. A previous study reported that WNT5A/ROR2 signaling can reduce bone density in early OA²⁹. Moreover, WNT5A inhibits anabolic gene expression and promotes MMP production in human chondrocytes²⁸. Our data along with these previous reports suggest that WNT5A and ROR2 expression levels were increased in OA cartilage and subchondral bone. Based on these findings, we infer that over-expression of WNT5A and ROR2 mainly causes cartilage destruction (because of the reduced Col-II and increased Caspase-3) and subchondral bone structure damage (mainly due to decreased BMD and increased SMI)^{28,29,44-46}. However, PTH (1-34) significantly down-regulates the expression of WNT5A and ROR2 in the development of OA, thereby preserving the cartilage and subchondral bone.

Conclusions

In the present study, PTH (1-34) was shown to prevent the further aggravation of cartilage degradation in a collagenase-induced OA model, and this beneficial effect on cartilage was accompanied by increases in subchondral bone mass and further protection of the subchondral micro-architecture from deterioration. The molecular mechanisms underlying the protective effect of PTH (1-34) on cartilage and subchondral bone may be the down-regulated expression of JAK2, STAT3, WNT5A, and ROR2.

Acknowledgments

Funding: The study was supported by the Natural Science Foundation of Hebei Province (H2016209176; H2019209550), the National Natural Science Foundation of China (NSFC 31671235 and 81874029), the Youth Talent Support Program of Hebei Province (JI-2016-10), and the 100 Innovative Talents Support Foundation of Hebei Province (JJK-2019-14). All authors thank Hong Xu for providing technical support during the data analysis.

Conflicts of Interest

The authors declare no conflicts of interest.

Ethical Approval

All procedures performed in studies involving animals were in accordance with the ethical standards of the institution or practice at which the studies were conducted. This study was approved by the Animal Ethical Committee of North China University of Science and Technology (LZ2019034).

References

- Gou Y, Tian F, Dai M, et al. Salmon calcitonin exerts better preventive effects than celecoxib on lumbar facet joint degeneration and long-term tactile allodynia in rats. *Bone*, 2019, 127: 17–25.
- Goldring MB, Goldring SR. Articular cartilage and subchondral bone in the pathogenesis of osteoarthritis. *Ann N Y Acad Sci*, 2010, 1192: 230–237.
- Wang Y, Fan X, Xing L, et al. Wnt signaling: a promising target for osteoarthritis therapy. *Cell Commun Signal*, 2019, 17: 97.
- Bailey AJ, Mansell JP. Do subchondral bone changes exacerbate or precede articular cartilage destruction in osteoarthritis of the elderly? *Gerontology*, 1997, 43: 296–304.
- Ding M, Odgaard A, Hvid I. Changes in the three-dimensional microstructure of human tibial cancellous bone in early osteoarthritis. *J Bone Joint Surg Br*, 2003, 85: 906–912.
- Dai MW, Chu JG, Tian FM, et al. Parathyroid hormone(1-34) exhibits more comprehensive effects than celecoxib in cartilage metabolism and maintaining

subchondral bone micro-architecture in meniscectomized Guinea pigs. *Osteoarthritis Cartil*, 2016, 24: 1103–1112.

7. Yan JY, Tian FM, Wang WY, *et al*. Parathyroid hormone (1-34) prevents cartilage degradation and preserves subchondral bone micro-architecture in Guinea pigs with spontaneous osteoarthritis. *Osteoarthritis Cartil*, 2014, 22: 1869–1877.
8. Hayami T, Pickarski M, Zhuo Y, *et al*. Characterization of articular cartilage and subchondral bone changes in the rat anterior cruciate ligament transection and meniscectomized models of osteoarthritis. *Bone*, 2006, 38: 234–243.
9. Hayami T, Pickarski M, Wesolowski GA, *et al*. The role of subchondral bone remodeling in osteoarthritis: reduction of cartilage degeneration and prevention of osteophyte formation by alendronate in the rat anterior cruciate ligament transection model. *Arthritis Rheum*, 2004, 50: 1193–1206.
10. Chen Y, Hu Y, Yu YE, *et al*. Subchondral trabecular rod loss and plate thickening in the development of osteoarthritis. *J Bone Miner Res*, 2018, 33: 316–327.
11. Henak CR, Kapron AL, Anderson AE, *et al*. Specimen-specific predictions of contact stress under physiological loading in the human hip: validation and sensitivity studies. *Biomech Model Mechanobiol*, 2014, 13: 387–400.
12. Burr DB, Gallant MA. Bone remodelling in osteoarthritis. *Nat Rev Rheumatol*, 2012, 8: 665–673.
13. Maldonado M, Nam J. The role of changes in extracellular matrix of cartilage in the presence of inflammation on the pathology of osteoarthritis. *Biomed Res Int*, 2013, 2013: 284873.
14. Lin EA, Liu CJ. The role of ADAMTSs in arthritis. *Protein Cell*, 2010, 1: 33–47.
15. Thomas CM, Fuller CJ, Whittles CE, *et al*. Chondrocyte death by apoptosis is associated with the initiation and severity of articular cartilage degradation. *Int J Rheum Dis*, 2011, 14: 191–198.
16. Xu Y, Dai GJ, Liu Q, *et al*. Sanmiao formula inhibits chondrocyte apoptosis and cartilage matrix degradation in a rat model of osteoarthritis. *Exp Ther Med*, 2014, 8: 1065–1074.
17. Chang JK, Chang LH, Hung SH, *et al*. Parathyroid hormone 1-34 inhibits terminal differentiation of human articular chondrocytes and osteoarthritis progression in rats. *Arthritis Rheum*, 2009, 60: 3049–3060.
18. Orth P, Cucchiariini M, Zurakowski D, *et al*. Parathyroid hormone [1-34] improves articular cartilage surface architecture and integration and subchondral bone reconstitution in osteochondral defects in vivo. *Osteoarthritis Cartil*, 2013, 21: 614–624.
19. Liu CC, Kalu DN. Human parathyroid hormone-(1-34) prevents bone loss and augments bone formation in sexually mature ovariectomized rats. *J Bone Miner Res*, 1990, 5: 973–982.
20. Harrington EK, Coon DJ, Kern MF, *et al*. PTH stimulated growth and decreased col-X deposition are phosphatidylinositol-3,4,5 triphosphate kinase and mitogen activating protein kinase dependent in avian sterna. *Anat Rec*, 2010, 293: 225–234.
21. Yavropoulou MP, Michopoulos A, Yovos JG. PTH and PTHR1 in osteocytes. New insights into old partners. *Hormones (Athens)*, 2017, 16: 150–160.
22. Wein MN, Kronenberg HM. Regulation of bone remodeling by parathyroid hormone. *Cold Spring Harb Perspect Med*, 2018, 1: 8–16.
23. Wu X, Cao L, Li F, Ma C, *et al*. Interleukin-6 from subchondral bone mesenchymal stem cells contributes to the pathological phenotypes of experimental osteoarthritis. *Am J Transl Res*, 2018, 10: 1143–1154.
24. Yao ZZ, Hu AX, Liu XS. DUSP19 regulates IL-1beta-induced apoptosis and MMPs expression in rat chondrocytes through JAK2/STAT3 signaling pathway. *Biomed Pharmacother*, 2017, 96: 1209–1215.
25. Bei M, Tian F, Liu N, *et al*. A novel rat model of Patellofemoral osteoarthritis due to patella Baja, or low-lying patella. *Med Sci Monit*, 2019, 25: 2702–2717.
26. Huang CY, Lai KY, Hung LF, *et al*. Advanced glycation end products cause collagen II reduction by activating Janus kinase/signal transducer and activator of transcription 3 pathway in porcine chondrocytes. *Rheumatology*, 2011, 50: 1379–1389.
27. Hosseini-Farahabadi S, Geetha-Loganathan P, Fu K, Nimmagadda S, *et al*. Dual functions for WNT5A during cartilage development and in disease. *Matrix Biol*, 2013, 32: 252–264.
28. Huang G, Chubinskaya S, Liao W, Loeser RF. Wnt5a induces catabolic signaling and matrix metalloproteinase production in human articular chondrocytes. *Osteoarthritis Cartil*, 2017, 25: 1505–1515.
29. Maeda K, Kobayashi Y, Udagawa N, *et al*. Wnt5a-Ror2 signaling between osteoblast-lineage cells and osteoclast precursors enhances osteoclastogenesis. *Nat Med*, 2012, 18: 405–412.
30. ter Huurne M, Schelbergen R, Blattes R, *et al*. Antiinflammatory and chondroprotective effects of intraarticular injection of adipose-derived stem cells in experimental osteoarthritis. *Arthritis Rheum*, 2012, 64: 3604–3613.
31. Kraus VB, Huebner JL, DeGroot J, *et al*. The OARSI histopathology initiative - recommendations for histological assessments of osteoarthritis in the Guinea pig. *Osteoarthritis Cartil*, 2010, 3: 35–52.
32. Little CB, Smith MM, Cake MA, *et al*. The OARSI histopathology initiative - recommendations for histological assessments of osteoarthritis in sheep and goats. *Osteoarthritis Cartil*, 2010, 3: 80–92.
33. van der Kraan PM, Vitters EL, van Beuningen HM, *et al*. Degenerative knee joint lesions in mice after a single intra-articular collagenase injection. A new model of osteoarthritis. *J Exp Pathol (Oxford)*, 1990, 71: 19–31.
34. van Osch GJ, van der Kraan PM, Vitters EL, *et al*. Induction of osteoarthritis by intra-articular injection of collagenase in mice. Strain and sex related differences. *Osteoarthritis Cartil*, 1993, 1: 171–177.
35. Pearle AD, Warren RF, Rodeo SA. Basic science of articular cartilage and osteoarthritis. *Clin Sports Med*, 2005, 24: 1–12.
36. Chen Q, Zhang B, Yi T, Xia C. Increased apoptosis in human knee osteoarthritis cartilage related to the expression of protein kinase B and protein kinase Cα in chondrocytes. *Folia Histochem Cytobiol*, 2012, 50: 137–143.
37. Huang JG, Xia C, Zheng XP, *et al*. 17beta-estradiol promotes cell proliferation in rat osteoarthritis model chondrocytes via PI3K/Akt pathway. *Cell Mol Biol Lett*, 2011, 16: 564–575.
38. Zhang XH, Xu XX, Xu T. Ginsenoside Ro suppresses interleukin-1beta-induced apoptosis and inflammation in rat chondrocytes by inhibiting NF-kappaB. *Chin J Nat Med*, 2015, 13: 283–289.
39. Bellido M, Lugo L, Roman-Blas JA, *et al*. Subchondral bone microstructural damage by increased remodelling aggravates experimental osteoarthritis preceded by osteoporosis. *Arthritis Res Ther*, 2010, 12: 152–156.
40. Behera AK, Thorpe CM, Kidder JM, *et al*. Borrelia burgdorferi-induced expression of matrix metalloproteinases from human chondrocytes requires mitogen-activated protein kinase and Janus kinase/signal transducer and activator of transcription signaling pathways. *Infect Immun*, 2004, 72: 2864–2871.
41. Legendre F, Bogdanowicz P, Boumediene K, *et al*. Role of interleukin 6 (IL-6)/IL-6R-induced signal transducers and activators of transcription and mitogen-activated protein kinase/extracellular. *J Rheumatol*, 2005, 32: 1307–1316.
42. Zhu J, Tang Y, Wu Q, *et al*. HIF-1alpha facilitates osteocyte-mediated osteoclastogenesis by activating JAK2/STAT3 pathway in vitro. *J Cell Physiol*, 2019, 234: 21182–21192.
43. Liu J, Cao L, Gao X, *et al*. Ghrelin prevents articular cartilage matrix destruction in human chondrocytes. *Biomed Pharmacother*, 2018, 98: 651–655.
44. Usami Y, Gunawardena AT, Iwamoto M, *et al*. Wnt signaling in cartilage development and diseases: lessons from animal studies. *Lab Invest*, 2016, 96: 186–196.
45. Luyten FP, Tylzanowski P, Lories RJ. Wnt signaling and osteoarthritis. *Bone*, 2009, 44: 522–527.
46. Li Y, Xiao W, Sun M, *et al*. The expression of Osteopontin and Wnt5a in articular cartilage of patients with knee osteoarthritis and its correlation with disease severity. *Biomed Res Int*, 2016, 2016: 9561058.